GEOPHYSICAL RESEARCH LETTERS, VOL. 26, NO. 22, PAGES 3397-3400, NOVEMBER 15, 1999

First Results from the Hawaiian SWELL Pilot Experiment

G. Laske, J. Phipps Morgan and J.A. Orcutt

IGPP, Scripps Institution of Oceanography, University of California San Diego

Abstract. In a year-long pilot experiment to the southwest of the Hawaiian Islands, we recorded teleseismic intermediate-period Rayleigh waves on ocean-bottom "L-CHEAPO" instruments using differential pressure gauges as sensors. We analyzed over 70 events and obtained accurate phase velocity estimates at periods between 15 and 70s. The average seismic structure beneath the pilot array does not deviate significantly from a standard seismic model of 100 Myr old oceanic lithosphere. However, we find strong lateral velocity variations across the array with large negative anomalies appearing within roughly 300km of the island chain. We are able to image the edge of the Hawaiian Swell and hence demonstrate the importance of making phase velocity measurements on the ocean floor.

Introduction

Several years ago we proposed to greatly improve seismic constraints on the support of Hawaiian swell relief by recording Rayleigh waves at periods 15-80 s at a large array of ocean-bottom instruments (Figure 1). The primary objective of the SWELL experiment (Seismic Wave Exploration of the Lower Lithosphere) is to image the lithosphere and upper asthenosphere system. While regional surface wave studies, using temporary broad-band arrays, are commonly used to map lithospheric and asthenospheric structure beneath continents (e.g. *Zielhuis and van der Hilst*, 1996], such studies have been extremely rare in the oceans. In fact, such studies are only now starting to appear in the literature, after the successful completion of the MELT (Mantle Electromagnetic and Tomography) experiment [*Forsyth et al.*, 1998]. One of the main reasons for the lack of such studies is that traditional ocean-bottom instrumentation has not allowed seismologists to record deep-reaching surface waves with high fidelity. Our recently developed L-CHEAPO (Low–Cost Hardware for Earth Applications and Physical Oceanography) instruments enable us to record surface waves in the period-band of interest during a roughly year-long deployment, for a reasonable cost.

In 1997, we received NSF funding to conduct a "proof-of-concept" pilot study in a small region near OSN1 at ODP borehole 843B (Figure 1). The proximity to OSN1 provides an excellent opportunity to compare our data with broad-band marine data collected by more sophisticated and expensive borehole and seafloor inertial instruments [*Vernon et al.*, 1998]. For the SWELL pilot study, 8 L-CHEAPO instruments using DPG sensors (differential pressure gauges) were placed in a hexagonal array to the southwest of the Hawaiian Islands. The most important issues to be resolved by the pilot study were (1) Is a 12-month experiment long enough to yield sufficient azimuthal data coverage? (2) Is the instrumentation appropriate for recording long-period surface waves (> 50s) necessary to resolve structure beneath the lithosphere (> 80km)? (3) How accurately can we measure surface wave dispersion?

The pilot deployment was successfully completed in May 1998. The data lets us not only determine a preliminary 1-dimensional model of the structure beneath the pilot array (which was the primary scientific objective of the pilot study), but the excellent data quality and volume also allow us to study the 3-dimensional fine-scale structure in greater detail.

The field program and the data collected

The field program lasted from April 1997 to May 1998 (including one redeployment cruise in December 1977) and our database now includes 12.5 months of continuous data, sampled at 25Hz. Our experimental design worked out extremely well in many respects: 1) We collected numerous events with a very good signal-to-noise level and our surface wave database currently includes high-quality waveforms from 75 shallow teleseismic events. The azimuthal data coverage is as good as any 1-year deployment could achieve (Figure 2). 2) For most of the 75 events, we were able to measure the dispersion at periods between 17 and 50s. The high quality of the waveforms for some events allowed us to extend the analysis to 70s, sometimes even beyond that. Regarding the

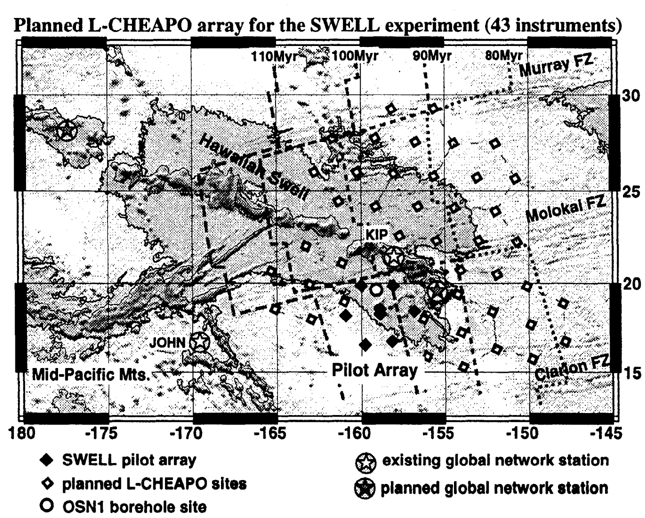

Figure 1. Location map for the planned SWELL experiment. The Hawaiian Swell is the region of shallow bathymetry (grey shade is bathymetry < 5 km). The instrument spacing of the pilot array was about 210km. Two instruments were placed near the center of the hexagon, 25 km apart. Also marked are the colocated ocean seismic network pilot borehole OSN1 and permanent existing (KIP, Kipapa and JOHN, Johnston Island) and planned (POHA, Hawaii and Midway) broad-band stations of the global seismic networks. Dashed lines mark the age of the ocean floor [*Müller et al.*, 1997].

Paper number 1999GL005401.
0094-8276/99/1999GL005401$05.00

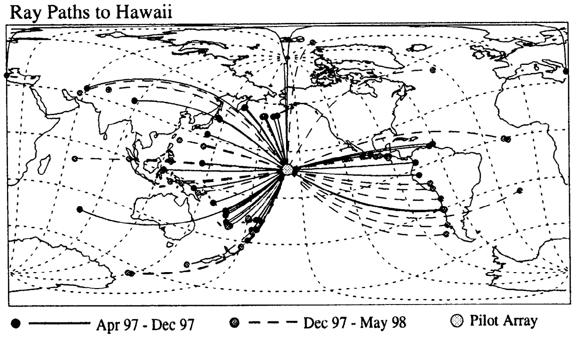

Figure 2. Data coverage for the two SWELL pilot deployments. We have inspected 40 shallow events of the first deployment and 35 shallow events of the second deployment (surface wave magnitude $M_S \geq 5.5$).

bandwidth, our dataset is extremely competitive with that of the recent MELT experiment [*Forsyth et al.*, 1998]. 3) The long-term deployment in the deep-sea environment provided an opportunity to test the reliability of the L-CHEAPO instruments and gain insight into possible improvements for future experiments of this kind.

A data example is shown in Figure 3. Though the section for the Rat Islands event has an very good signal-to-noise ratio, such records are not the exception in our dataset. Great waveform coherency across the array, as is apparent for the Rat Islands event, is very common. In fact, if waveform distortions occur, they are typically found on all seismograms across the array and can be explained by either the source mechanism or structure far from the pilot array (e.g. a segment of continental propagation).

Phase measurements across the pilot array

The standard analysis of surface wave dispersion involves 3 steps: a) measure the frequency-dependent phase, b) determine phase velocity (local or path-averaged), c) invert phase velocities for depth-dependent structure. For each event, we perform step a) by measuring the phase at one station with respect to that of all the others, using a multi-taper transfer function technique [*Laske and Masters*, 1996]. The phase measured for that station, for each event, is then the statistical average of all individual measurements. Our technique currently allows us to measure the phase with the required accuracy for event magnitudes down to Ms=5.5.

In step b) we determine average phase velocities across the array for each event using a multi-parameter least-squares procedure similar to that of *Stange and Friederich* [1993]. We fit spherical incoming wavefronts to all phase measurements, at each frequency. A free parameter we solve for is the frequency-dependent arrival angle. This accounts for the fact that lateral heterogeneity between source and receiver has diverted the wave packets from the source-receiver great circle. Occasionally, we measure off-great circle arrival angles of up to 15°. While this parameter does not immediately contribute to determining the structure within the array, including it in the modeling process is essential to obtain accurate phase velocity curves. We are aware that fitting simple wave fronts to phase measurements could lead to a biased phase velocity curve if the incoming wavefield has a strongly non-planar geometry. We find that events occurring in the North Atlantic, Indian Ocean or Eurasia do show distorted waveforms at the pilot array. Such events are associated with

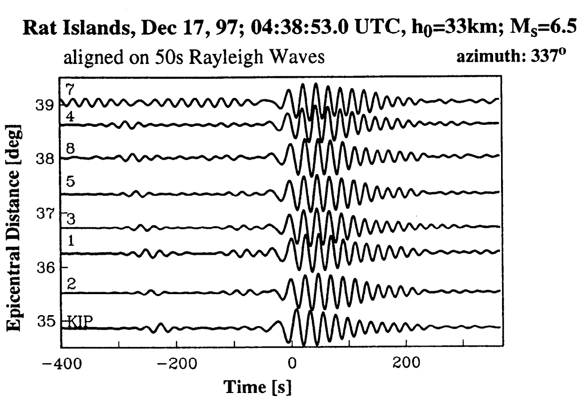

Figure 3. A data examples for the Rat Islands event. The waveforms are bandpass filtered between 0.015 and 0.05 Hz. Also shown are the waveforms of the vertical seismometer at station KIP. The records are *not* corrected for instrumental effects and the seismometer data have not been converted to pressure, hence perceived phase shifts may not be 'real'.

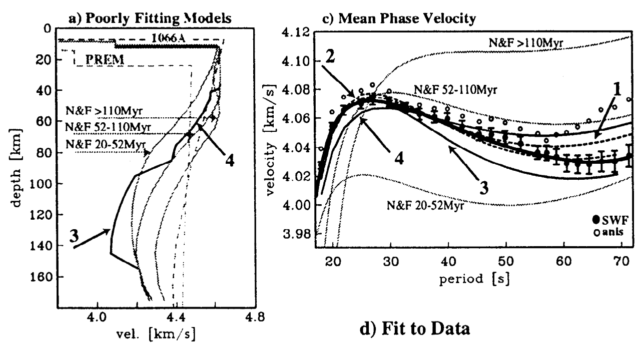

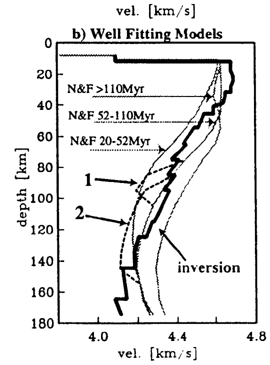

d) Fit to Data

Model	%	depth	thickness	Misfit (χ^2/N)
starting model: N&F 52-110				16.1
1	-3	90	20	2.4
2	-2	120	60	1.7
3	-3	120	60	6.1
4	-1	60	40	6.8
model from inversion				0.3
PREM				1695
1066a				569
N&F > 110				727
N&F 20-52				132

Figure 4. 1D shear velocity models that yield poor (4a) and acceptable (4b) fits to our data. The models of age-dependent oceanic lithosphere of *Nishimura and Forsyth* [1989] are given as reference (solid grey lines). Also marked are isotropic 1D reference Earth models PREM [*Dziewonski and Anderson,* 1981] and 1066a [*Gilbert and Dziewonski,* 1975] which are inconsistent with our data. Labels 1-4 mark models from the hypothesis test.
c) Observed phase velocity obtained from spherical wave fitting (SWF) (incl. 1-sigma error bars) and from modeling azimuthal anisotropy (anis). Also shown are predictions from the N&F models of Figure 4a. The phase velocity curve for 1066A increases with period (from 4.06km/s at 70s to 3.91km/s at 20s) and is not shown. Also omitted is the curve for PREM which is lower than that of 1066A by 0.04km/s on average.
d) Model parameters (magnitude of low velocity anomaly, its center and thickness) and the misfit of the data for the models obtained in the hypothesis test and in the inversion.

waves traveling across large continental areas and are discarded from our study. The great majority of the remaining events are circum-Pacific (Figure 2). The good coherency of the waveforms across the array for these events suggests that a spherically shaped wavefront is the only perturbation to the plane-wave case that we have to consider. For this study, we use high-quality phase velocity curves obtained for 50 events.

Average structure beneath the pilot array

The results from the spherical wavefront fitting process (SWF hereafter) are averaged to determine a 'reference phase velocity curve' that describes the mean dispersion across the array (Figure 4c). If strong lateral heterogeneity is present, such a dispersion curve gives a very crude estimate of the underlying structure. It is, however, a useful tool to evaluate the quality of our results and to obtain an estimate of the long-wavelength component of regional heterogeneity. A main objective of the pilot study is to determine if our results are precise enough to distinguish between signals associated with lithosphere of different age [*Nishimura and Forsyth,* 1989]. In particular, we would like to confirm or rule out a possible thinning of the swell lithosphere that is caused by 'rejuvenation' to an age of 25 Myr [*Detrick and Crough,* 1978]. At periods shorter than 50 s, the measured dispersion roughly follows that for 52-110 Myr old lithosphere (Figures 4a and 4b) and our data are clearly inconsistent with a model for oceanic lithosphere that is younger than that. On the other hand, at periods longer than 50s the measured dispersion is obviously lower than the predictions for 52-110Myr. This suggests a low velocity zone at greater depth, since the data at short periods do not allow a significant reduction in velocity at depths shallower than roughly 70 km. In a hypothesis test we investigate whether a low velocity layer can explain our observations. We determine the best-fitting models in a grid search where the center of the layer, layer thickness and the magnitude of the shear-velocity anomaly are free parameters. Pertubations in v_p and density are scaled using the standard scaling relationships $d\ln v_s/d\ln v_p = 1.7$ and $d\ln v_s/d\ln\rho = 2.5$. Using the average bathymetry at the array, Nishimura and Forsyth's model for 52-110 Myr serves as a starting model. The best–fitting models are model 1 (deep thick LVZ) and model 2 (shallower thin LVZ) though the data are barely fit ($\chi^2/N > 1$). The non-uniqueness of

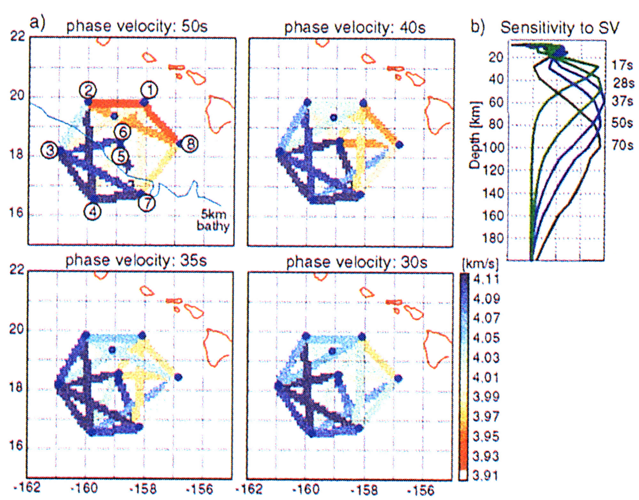

Figure 5. a) Variation of apparent phase velocity, as a function of period. Each line segment shows path-averaged velocities between pairs of stations. The most prominent feature is a velocity gradient towards the island chain that becomes stronger with increasing period.
b) S-velocity depth sensitivity kernels for Rayleigh wave phase velocity, as function of period.

our dataset allows a weak trade-off between the magnitude of the low-velocity anomaly and its depth extent (Figure 4). Models 3 (deep strong LVZ) and 4 (shallow weak LVZ) cannot fit our data adequately and mark bounds on the group of likely models. None of the models fit all data simultaneously which implies that a LVZ is not the only perturbation to the starting model that is required. We therefore also perform a smoothed inversion for shear velocity in 17 layers of variable thickness. The resulting model, that actually overfits the data, exhibits moderate undulations around the starting model. The most prominent features are increased velocities in the upper lithosphere, reduced velocities (but no true LVZ) in the lower lithosphere and significantly reduced velocities in the asthenosphere below 130 km depth. Although the resolution at these depths is relatively poor and the upper boundary of the low velocity layer may vary, its presence is required to fit the long-period data. There is a trade-off between the high-velocity lid at the top, which is a stable feature, and the undulations further down but the final model does not depend on the starting model.

Possible Bias from Azimuthal Anisotropy

We have also investigated the azimuthal dependence of phase velocity and the possible implications for anisotropic structure at depth (manuscript in preparation). Azimuthal anisotropy in phase velocity is commonly described by a truncated trigonometric power series [*Smith and Dahlen,* 1973] where the zeroth order term (named c_i hereafter) describes the azimuthally averaged (or isotropic) component. In the case of adequate data coverage, this term should be consistent with the average phase velocity we obtain from the SWF procedure. Any inconsistency implies that uneven data coverage could lead to bias in the results obtained from the SWF process. Figure 4c shows that the results from both techniques are indeed consistent at periods shorter than 60 s (the errors in the c_i's are typically twice that of the SWF errors). These data impose strong constraints on the seismic structure at depths less than roughly 100 km. At periods longer than 60s, the phase velocities obtained from the two techniques disagree so there is a bias in at least one of the two results. The number of reliable estimates decreases with increasing period (i.e. 50 measurements at 25s vs. 15 measurements at 67s). The corresponding poorer data coverage may allow a few high-quality low phase velocity values to dominate the SWF process and incorrectly implying the deep low-velocity anomaly discussed above. On the other hand, the results obtained from modeling azimuthal anisotropy at long periods are highly uncertain. The lack of data gives very unrealistic large-magnitude azimuthal anisotropy, allowing a shift in the c_i's toward higher values. Our conclusion is that the SWF results are more accurate and that our data are marginally consistent with an 'old' lithosphere/asthenosphere system but that they suggest a reduction in velocity at depths 130 km or greater.

Lateral variations across the pilot array

Perhaps one of the most intriguing results from the pilot study is that we find lateral heterogeneity across the array (Figure 5). A dispersion analysis along two-station legs reveals a strong velocity gradient that is roughly normal to the swell axis. Anomalously low velocities are found closer to the islands while higher velocities are found in the deep ocean. The velocities along individual legs are generally well constrained as the typical number of events per leg is 5 or greater. Note that parallel legs (e.g. 1-8, 3-4) have very different phase velocities, hence these observations cannot be explained by effects due to bias from azimuthal anisotropy. The velocity gradient becomes stronger with increasing period. At 50s, phase velocity perturbations across the array reach $\pm$ 2.5%. The good correlation with the bathymetry suggests that our results are strongly influenced by changes in water depth. However, this effect can be ruled out, since the signal has the wrong sign; increasing water depth decreases velocities and affects shorter periods more strongly. Variations in crustal structure is also an unlikely candidate as a thicker crust (as found in the immediate vicinity of the islands) greately decreases phase velocities at the short periods. The increase of the anomaly with increasing period points toward a low-velocity anomaly at greater depth (> 80 km), close to the island chain. This indicates that the low-velocity zone we found in the 1D modeling is indeed real. A detailed interpretation in terms of 3D velocity variations is underway. Initial inversion results suggest that the structure close to the islands is consistent with that of a 20-52 Myr old lithosphere/asthenosphere system while the lower lithosphere and asthenosphere (depths greater than 80 km) is anomalously fast beneath the deep ocean [*Laske et al.*, 1999]. We conclude from this that thermal rejuvenation [*Detrick and Crough,* 1978] clearly plays a role in the formation of the Hawaiian Swell but its seismic signature is lost 350 km away from the islands.

Discussion

Several mechanisms have been proposed to play a role in swell generation each of which is characterized by distinct seismic responses: (1) Thermal reheating (rejuvenation) of the lithosphere [*Crough,* 1978; *Detrick and Crough,* 1978] yields slow seismic velocities in the lower lithosphere (30-80km depth), (2) Compositional underplating of depleted mantle residue from hotspot melting [*Robinson,* 1988; *Phipps Morgan et al.*, 1995] produces relatively unchanged lithosphere and an anomalously *fast* sub–lithosphere (depths > 80km). A third mechanism expected to be found along the Hawaiian island chain is the dragging of hot plume asthenosphere by the overriding lithosphere [*Davies,* 1988; *Olson,* 1990; *Sleep,* 1990], a process which produces relatively unchanged lithosphere but seismically *slow* sublithospheric structure (depths > 80km). Our results support the idea that the lithosphere is thermally affected near the island chain by passage over the hotspot. Thermal rejunvenation thus plays a role in the formation of the Hawaiian Swell, but its geographic extent does not include the entire area of the SWELL pilot array. Anomalously fast phase velocities found in the deep ocean are evidence that compositional underplating may also be involved.

Our dataset does not allow us to speculate further on details of the Hawaiian Swell formation as the pilot array barely covers the edge of the swell. However, the discovery of lower velocities close to the islands is consistent with recent findings of the land-based experiments of *Wolfe et al.* [1998] and *Priestley and Tilmann* [1999]. The results of the pilot experiment are very encouraging and we believe that the dataset of the entire SWELL experiment will be an extremely rich one for studying the complexity of swell formation and the aspects of plume-lithosphere interaction and small-scale convection associated with it.

Acknowledgments. We thank the OBS team at IGPP for making this experiment possible. GEOSCOPE provided the data for station KIP. Thanks also to Jeroen Ritsema and an anonymous reviewer for helpful comments. This research was financed by National Science Foundation grants OCE-95-29707 and EAR-97-06056.

References

Crough, T., Thermal Origin of Hotspot Swells, *Geophys. J.R. Astr. Soc., 55* 451–469, 1978.

Davies, G.F., Ocean bathymetry and mantle convection, 1, large-scale flow and hotspots, *J. Geophys. Res., 93,*10,467–10,480, 1988.

Detrick, R.S., and S.T. Crough, Island subsidence, hot spots, and lithospheric thinning, *J. Geophys. Res., 83,* 1236–1244, 1978.

Dziewonski, A.M., and D.L. Anderson, Preliminary reference Earth model, *Phys. Earth Planet. Int., 25,* 297–356, 1981.

Forsyth, D.W., Webb, S.C., Dorman, L.M., and Y. Shen, Phase Velocities of Rayleigh Waves in the MELT Experiment on the East Pacific Rise, *Science, 280,* 1235–1238, 1998.

Gilbert, F.J., and A.M. Dziewonski, An Application of Normal Mode Theory to the Retrieval of Structural Parameters and Source Mechanisms from Seismic Spectra, *Phil. Trans. Roy. Soc. Lond., 278A,* 187–269, 1975.

Laske, G., and G. Masters, Constraints on global phase velocity maps by long-period polarization data, *J. Geophys. Res., 101,* 16,059–16,075, 1996.

Laske, G., J. Phipps Morgan, J., and J. Orcutt, Results from the Hawaiian SWELL Pilot experiment, *Proceedings of the IUGG99 General Assembly, Birmingham, England,* 1999.

Müller, R.D., Roest, W.R., Royer, J.-Y., Gahagan, L.M., and J.G. Sclater, Digital isochrons of the world's ocean floor, *J. Geophys. Res., 102,* 3211–3214, 1997.

Nishimura, C.E., and D.W. Forsyth, The anisotropic structure of the upper mantle in the Pacific, *Geophys. J., 96,* 203–229, 1989.

Olson, P., Hot Spots, Swells and Mantle Plumes, in *Magma Transport and Storage*, edited by M.P. Ryan, John Wiley, New York, 33–51, 1990.

Phipps Morgan, J., Morgan, W.J., Zhang, Y.-S., and W.H.F. Smith, Observational hints for a plume-fed, suboceanic asthenosphere and its role in mantle convection, *J. Geophys. Res., 100,* 12,753–12,767, 1995.

Priestley, K., and R. Tilmann, Shear-wave structure of the lithosphere above the Hawaiian hot spot from two-station Rayleigh wave phase velocity measurements, *Geophys. Res. Lett., 26,* 1493–1496, 1999.

Robinson, E.M., The topographic and gravitational expression of density anomalies due to melt extraction in the uppermost oceanic mantle, *Earth Planet. Sci. Lett., 90,* 221–228, 1998.

Sleep, N.H., Hotspots and Mantle Plumes: Some Phenomenology, *J. Geophys. Res., 95,* 6715–6736, 1990.

Smith, M.L., and F.A. Dahlen, The azimuthal dependence of Love and Rayleigh wave propagation in a slightly anisotropic medium, *J. Geophys. Res., 78* 3321–3333, 1973.

Stange, S. and W. Friederich, Surface wave dispersion and upper mantle structure beneath southern Germany from joint inversion of network recorded teleseismic events, *Geophys. Res. Lett., 20,* 2375–2378, 1993.

Vernon, F.L., Collins, J.A., Orcutt, J.A., Stephen, R.A., Peal, K., Wolfe, C.J., Hildebrand, J.A., and F.N. Spiess, Evaluation of Teleseismic Waveforms and Detection Thresholds From the OSN Pilot Experiment, *Eos Trans. AGU, 79,* F650, 1998.

Wolfe, C.J., Shen, Y., Solomon, S.C., and P.G. Silver, Initial results from the PELENET experiment along the Hawaiian Islands: Body wave delay times and P-to-S conversions at the 410- and 660-km discontinuities, *Eos Trans. AGU, 79,* S208, 1998.

A. Zielhuis, A., and R.D. van der Hilst, R.D., Upper-mantle shear velocity beneath eastern Australia from inversion of waveforms from SKIPPY portable arrays, *Geophys. J. Int., 127,* 1–16, 1996.

G. Laske, J. Phipps Morgan and J.A. Orcutt, IGPP, Scripps Institution of Oceanography, University of California San Diego, CA 92093-0225 (e-mail:glaske@ucsd.edu)

(Received June 22, 1999; revised September 21, 1999; accepted September 23, 1999.)